

## HELIUM MIXING IN GLOBULAR CLUSTER STARS

Allen V. Sweigart

Laboratory for Astronomy and Solar Physics, Code 681  
NASA/Goddard Space Flight Center, Greenbelt, MD 20771

ABSTRACT: The observed abundance variations in globular cluster red giants indicate that these stars may be mixing helium from the hydrogen shell outward into the envelope, presumably as a result of internal rotation. We have investigated the implications of such helium mixing for both the red-giant-branch (RGB) and horizontal-branch (HB) phases by computing a number of noncanonical evolutionary sequences for different assumed mixing depths and mass loss rates. We find that the helium-mixed models evolve to higher luminosities during the RGB phase and consequently lose more mass than their canonical counterparts. This enhanced mass loss together with the higher envelope helium abundances of the helium-mixed models produces a markedly bluer and somewhat brighter HB morphology. As a result, helium mixing can mimic age as a 2nd parameter and can reduce the ages of the metal-poor globular clusters derived from the luminosity difference between the HB and the main sequence turnoff. Helium mixing might also lead to a larger RR Lyrae period shift and to a steeper slope for the RR Lyrae luminosity - metallicity relation if the mixing is more extensive at low metallicities, as suggested by the observed abundance variations. We discuss the implications of helium mixing for a number of other topics including the low gravities of the blue HB stars, the origin of the extreme HB stars, and the evolutionary status of the sdO stars. A variety of observational tests are presented to test this helium-mixing scenario.

### 1. Introduction

Red-giant stars in individual globular clusters show large star-to-star variations in the abundances of C, N, O, Na and Al which are not predicted by canonical stellar evolution theory. These variations are often anticorrelated in a manner suggestive of nuclear processing and frequently become more pronounced with evolution up the red-giant branch (RGB), as shown, for instance, by the decline in the C abundance along the giant branches of M92 and NGC 6397 (Bell, Dickens, & Gustafsson 1979; Carbon et al. 1982; Briley et al.

1990) and by the presence of super O-poor stars near the tip of the RGB in M13 (Kraft et al. 1993, 1997). These observational results indicate that low-mass red giants are capable of mixing nuclearly processed material from the vicinity of the hydrogen shell out to the surface (Kraft 1994). Although the nature of the mixing process is not well understood, it is widely suspected that internal rotation plays a crucial role, perhaps via meridional circulation (Sweigart & Mengel 1979; Peterson 1983; Norris 1987; Kraft 1994).

The observed variations of Al (e. g., Norris & Da Costa 1995; Kraft et al. 1997) are particularly important because they require the deepest penetration of the mixing currents. Langer, Hoffman, & Sneden (1993) have shown that Al can be produced in low-mass red giants via proton captures on Mg, but this seems to occur only within the hydrogen shell (Langer & Hoffman 1995; Cavallo, Sweigart, & Bell 1996, 1997). *Thus any mixing process which dredges up Al will also dredge up helium.* Since the helium abundance is one of the main parameters determining the stellar structure, such mixing could potentially have a major impact on the luminosities, effective temperatures and lifetimes of the subsequent evolutionary phases, especially the horizontal-branch (HB) phase (Langer & Hoffman 1995; Sweigart 1997).

We have computed a number of noncanonical evolutionary sequences in order to investigate the consequences of mixing helium from the hydrogen shell into the envelope of a globular cluster red-giant star (Sweigart 1997). We describe these RGB sequences as well as the numerical algorithm for helium mixing in the following section. The main results are given in Sec. 3, where we briefly explore the implications of helium mixing for four topics, namely, the morphology of the HB and the 2nd parameter effect, the low gravities of the blue HB (BHB) stars, the origin of the extreme HB (EHB) stars, and the evolutionary status of the helium-rich sdO stars. A short summary is given in Sec. 4.

## 2. RGB Evolutionary Sequences with Helium Mixing

We first discuss the composition distribution around the hydrogen shell of a typical RGB model in order to emphasize the connection between the observed Al enhancements and helium mixing. Figure 1 gives a representative distribution taken from the results of Cavallo et al. (1997). Although the details of the composition distribution in Figure 1 can vary somewhat from case to case, the main features should be invariant. In particular, we note that there is a region above the hydrogen shell within which C is depleted by the CN cycle and, somewhat closer to the shell, a region within which O is depleted by the ON cycle. The dredge-up of CN and ON processed material from these regions would alter the envelope CNO abundances even if the mixing currents do not penetrate into the shell. Thus the observed CNO variations by themselves do not necessarily imply helium mixing.

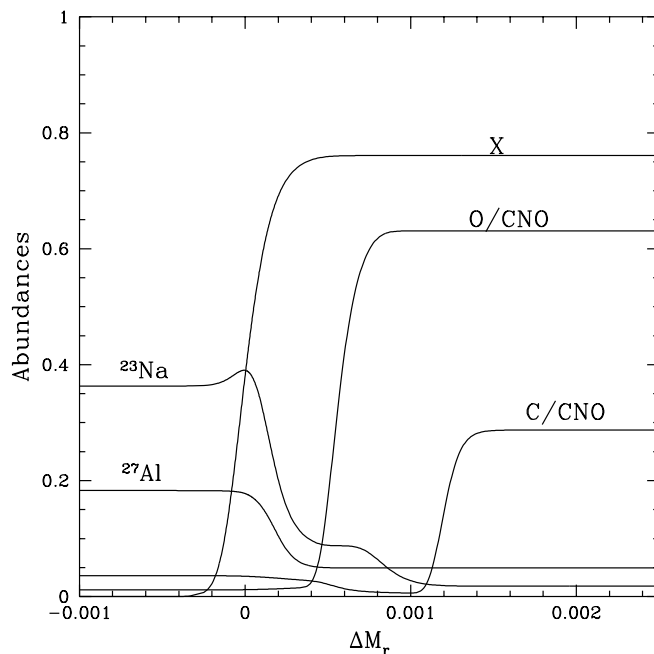


Fig. 1.— Composition distribution around the hydrogen shell of a typical RGB model. The hydrogen shell is labeled by the hydrogen abundance  $X$ . The C and O abundances are given as fractions of the total CNO abundance, while the  $^{23}\text{Na}$  and  $^{27}\text{Al}$  abundances have been multiplied by factors of 10 and 20, respectively. The abscissa gives the difference in the mass coordinate  $M_r$  in solar units relative to the center of the shell.

The same is also true for  $^{23}\text{Na}$  which is enhanced above the shell by proton capture on  $^{22}\text{Ne}$ , although larger  $^{23}\text{Na}$  enhancements would require mixing into the shell where proton capture on the more abundant  $^{20}\text{Ne}$  can take place (Denisenkov & Denisenkova 1990). In contrast,  $^{27}\text{Al}$  is only produced within the shell because of the higher temperatures needed for proton capture by Mg. It follows therefore that the dredge-up of Al, as implied by the observations, will be accompanied by the dredge-up of helium. In some cases helium might be dredged up from the upper part of the shell, where Al is not always enhanced. Thus an enhancement in the surface Al abundance would be a sufficient, but not necessary, condition for helium mixing.

Helium mixing was included in the model calculations with the algorithm illustrated in Figure 2. We assume that the mixing currents are able to penetrate into the shell and consequently that some of the helium produced by the hydrogen burning is added to the envelope instead of the core. The depth of the mixing is specified by the parameter  $\Delta X_{\text{mix}}$  which measures the difference in the hydrogen abundance  $X$  between the envelope ( $X = X_{\text{env}}$ ) and the innermost point reached by the mixing currents ( $X = X_{\text{env}} - \Delta X_{\text{mix}}$ ).

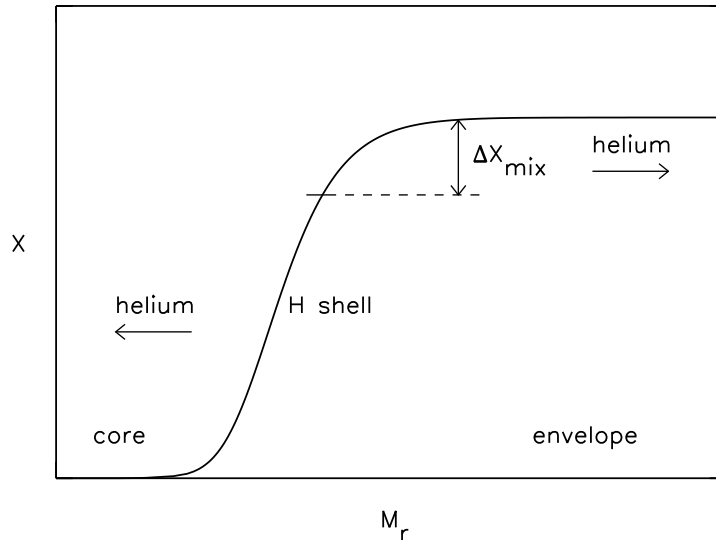


Fig. 2.— Schematic representation of the algorithm for helium mixing in RGB models. The solid curve gives the hydrogen abundance  $X$  within the hydrogen shell as a function of the mass coordinate  $M_r$ .

All of the helium produced outside the point where  $X = X_{\text{env}} - \Delta X_{\text{mix}}$  is mixed outward into the envelope where it is diluted throughout the entire envelope mass. As a result, the envelope hydrogen abundance gradually decreases from one model to the next. All of the helium produced interior to the point where  $X = X_{\text{env}} - \Delta X_{\text{mix}}$  is added to the core as in canonical models. For simplicity we assume that the penetration depth  $\Delta X_{\text{mix}}$  is constant during the evolution up the RGB. This assumption will be relaxed in future computations.

Using this algorithm, we have evolved 53 sequences up the RGB to the helium flash for various amounts of helium mixing and mass loss. More specifically, we have computed sequences for  $\Delta X_{\text{mix}} = 0.0$  (no helium mixing), 0.05, 0.10 and 0.20 and for  $\eta_R = 0.0$  (no mass loss) to 0.8, where  $\eta_R$  is the Reimers (1975) mass loss parameter introduced by Fusi Pecci & Renzini (1976). Helium mixing was begun at the point along the RGB where the hydrogen shell burns through the hydrogen discontinuity produced by the deep penetration of the convective envelope during the first dredge-up. This point corresponds to the well-known “bump” in the RGB luminosity function (Fusi Pecci et al. 1990 and references therein). Each sequence had the same mass and composition at the zero-age main sequence, i.e., mass  $M = 0.805 M_{\odot}$ , helium abundance  $Y = 0.23$  and heavy-element abundance  $Z = 0.0005$ . The input physics for these sequences is outlined by Sweigart (1997).

We emphasize that the results presented here are based on a single value of  $Z$  and on the mixing algorithm in Figure 2. Consequently they explore just a small part of parameter

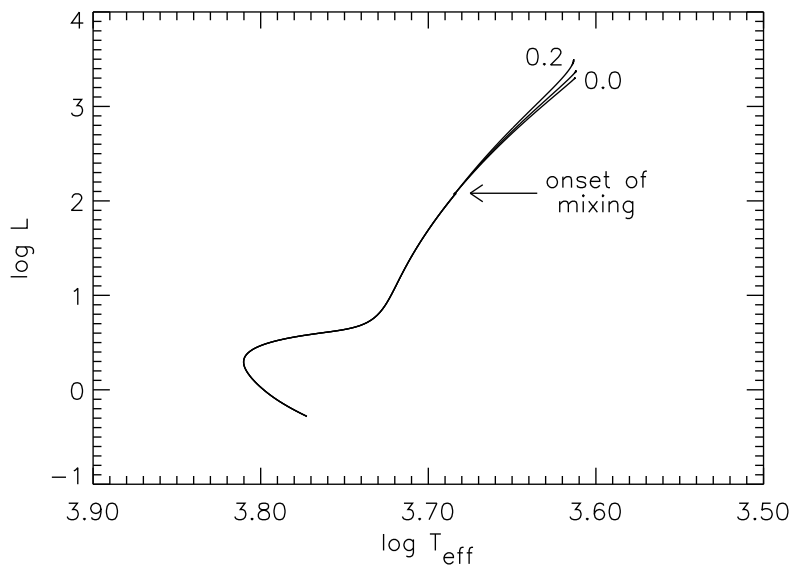


Fig. 3.— RGB evolutionary tracks for the Reimers mass loss parameter  $\eta_R = 0.3$  and 3 depths of helium mixing:  $\Delta X_{\text{mix}} = 0.0$  (canonical evolution), 0.1 and 0.2.

space. We will extend these preliminary results in future calculations, especially to higher metallicities.

With this caveat we now consider the effects of helium mixing on the RGB evolution. Figure 3 shows 3 RGB tracks computed for the mass loss parameter  $\eta_R = 0.3$ : a canonical track labeled by  $\Delta X_{\text{mix}} = 0.0$  and 2 helium-mixed tracks for  $\Delta X_{\text{mix}} = 0.1$  and 0.2. As indicated previously, helium mixing begins at the bump in the RGB luminosity function which in this case occurs at  $\log L = 2.1$ . Prior to this point the tracks in Figure 3 are identical. Helium mixing along the  $\Delta X_{\text{mix}} = 0.1$  and 0.2 tracks leads to a progressive increase in the envelope helium abundance  $Y_{\text{env}}$  (see Figure 2 of Sweigart 1997). By the tip of the RGB,  $Y_{\text{env}}$  in these sequences exceeds the canonical value by 0.07 and 0.19, respectively. Despite this substantial increase in  $Y_{\text{env}}$ , the helium-mixed and canonical tracks have quite similar morphologies. In particular, the helium-mixed tracks are shifted blueward by only a few 0.01 mag in  $B-V$ , which would be difficult to detect, given the paucity of stars near the tip of the RGB in the globular clusters.

One important consequence of helium mixing is an increase in the RGB tip luminosity. This occurs because the higher envelope helium abundance in the helium-mixed models affects both the hydrostatic structure around the hydrogen shell by increasing the mean molecular weight and the thermal structure by decreasing the opacity. Both of these effects act together to increase the hydrogen burning rate and hence the surface luminosity.

As a result, the helium-mixed sequences lose significantly more mass during the RGB phase for a given value of  $\eta_R$ , as illustrated in Figure 3 of Sweigart (1997). This suggests that a spread in the stellar rotation rate might lead to a spread in the final RGB mass, should rotation control the amount of helium mixing.

The correlation between the Al enhancement and the envelope helium abundance predicted by helium mixing implies that the Al-enhanced giants in a cluster such as M13 should appear to be more metal-rich than the Al-normal giants. The size of the predicted spread in  $[\text{Fe}/\text{H}]$  is, however, quite small, amounting to only 0.04 and 0.12, respectively, by the tip of the RGB in the  $\Delta X_{\text{mix}} = 0.1$  and 0.2 tracks in Figure 3. Although the detection of such a small spread in  $[\text{Fe}/\text{H}]$  would be a formidable undertaking, there are some factors which would reduce the observational uncertainties. Most importantly, this test depends on a differential, not absolute, measurement of  $[\text{Fe}/\text{H}]$ . Moreover, one could compare mean  $[\text{Fe}/\text{H}]$  values for the Al-enhanced and Al-normal giants.

### 3. Implications for HB and Post-HB Evolution

#### 3.1. Horizontal-Branch Morphology: 2nd Parameter Effect

In order to investigate the effects of helium mixing on the post-RGB evolution, we have continued all of the RGB sequences through the helium flash to the zero-age horizontal branch (ZAHB) and then through the HB and post-HB phases until the onset of the helium-shell flashes. Using these evolutionary sequences, we will now address four aspects of the HB and post-HB evolution, beginning with the morphology of the HB and the 2nd parameter effect.

From the previous discussion we know that a helium-mixed star will arrive on the ZAHB with a higher envelope helium abundance and a lower mass than the corresponding canonical star and hence will lie at a higher effective temperature. In fact, a star's ZAHB location turns out to be remarkably sensitive to the amount of helium mixing. We illustrate this point in Figure 4, where we present 4 synthetic HB simulations (Catelan 1996) for various amounts of helium mixing. The canonical simulation given in panel (a) assumes a Gaussian distribution of the HB mass  $M_{\text{HB}}$  with a mean mass  $\langle M_{\text{HB}} \rangle$  of  $0.675 M_{\odot}$ , corresponding to a mean mass loss parameter  $\langle \eta_R \rangle$  of 0.34, and a mass dispersion  $\sigma_M$  of  $0.03 M_{\odot}$ . These values were chosen to give an M3-like HB morphology with approximately equal numbers of stars blueward and redward of the instability strip, as indicated by the HB parameters (cf. Buonanno 1993) listed in the upper left corner of panel (a). The simulations in the remaining panels of Figure 4 then adopt the same distribution in  $\eta_R$  as implied by the mass distribution in panel (a).

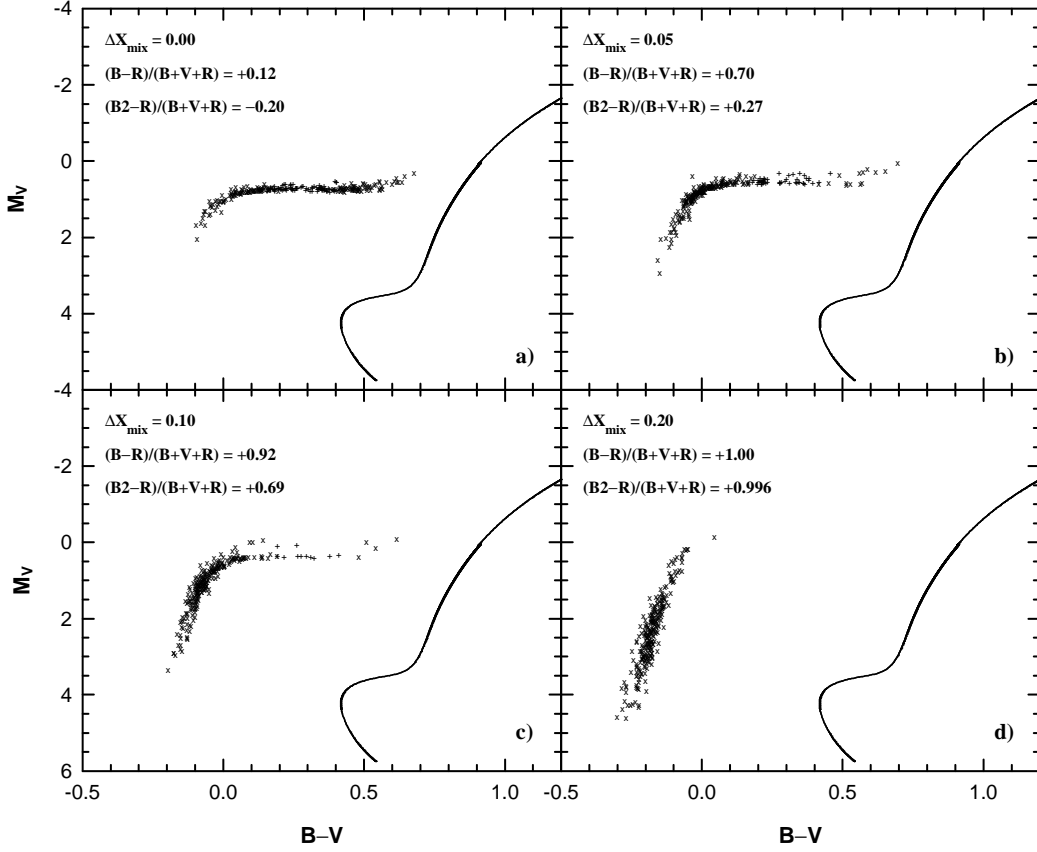


Fig. 4.— Synthetic HB simulations for canonical evolution (panel a) and for 3 depths of helium mixing:  $\Delta X_{\text{mix}} = 0.05$  (panel b), 0.10 (panel c) and 0.20 (panel d). Plus signs denote RR Lyrae variables.

The simulation in panel (b) for  $\Delta X_{\text{mix}} = 0.05$  shows that helium mixing leads to a markedly bluer HB morphology even though the mean increase in  $Y_{\text{env}}$  in this case is only  $\approx 0.03$ . Besides being bluer, the HB in panel (b) is also brighter by  $\approx 0.2$  mag, implying a corresponding increase in the luminosity difference  $\Delta V$  between the HB and the main sequence turnoff. It follows that the “apparent” age derived from the  $\Delta V$  method (e.g., Iben & Renzini 1984) for the cluster in panel (b) would be 2 - 3 Gyr older than for the canonical cluster in panel (a). This is approximately the age difference required to explain the change in the HB morphology between panels (a) and (b), assuming that age is the only parameter that varies between these clusters. By shifting the HB blueward and making the clusters appear older, helium mixing could therefore mimic age as a 2nd parameter. This would obviously affect estimates of the formation timescale of the galactic halo derived from the 2nd parameter clusters.

Besides affecting the relative ages of the 2nd parameter clusters, helium mixing could also affect the absolute globular cluster ages, particularly for the most metal-poor (and presumably oldest) clusters for which the observed abundance variations in CNO (Bell & Dickens 1980) and possibly Al (Norris & Da Costa 1995) are most pronounced. The fact that the most metal-poor globular clusters do not have the bluest HB's may be an indication that the mass loss efficiency decreases at the lowest metallicities (Renzini 1983; Fusi Pecci et al. 1993). The present sequences show that helium mixing increases the ZAHB luminosity  $L_{\text{HB}}$  near the instability strip at the rate  $\Delta \log L_{\text{HB}} \approx 1.5 \Delta X_{\text{mix}}$ . Combining this result with the dependence of the globular cluster age on the turnoff luminosity given, for example, by VandenBerg, Bolte, & Stetson (1996), we obtain the relationship

$$\Delta t \approx -50 \Delta X_{\text{mix}} \quad (1)$$

between the change in the globular cluster age in Gyr, as inferred from  $\Delta V$ , and the helium mixing parameter  $\Delta X_{\text{mix}}$ . We see that even a modest penetration of the mixing currents into the hydrogen shell during the RGB phase would significantly reduce the globular cluster age, as a consequence of the higher luminosity of the helium-mixed HB models. This may be especially important for clusters where the determination of  $\Delta V$  requires an extrapolation from the blue HB (see discussion by Buonanno, Corsi, & Fusi Pecci 1989). The ages estimated from  $\Delta V$  in such cases might be too large if mixing is responsible for the blue HB morphology. A possible example of this effect is the cluster M10, whose very blue HB seems to be unusually bright (Hurley, Richer, & Fahlman 1989; Arribas, Caputo, & Martinez-Roger 1991). Interestingly, the  $\Delta V$  value for M10 is the second largest in the sample of 43 clusters studied by Chaboyer, Demarque, & Sarajedini (1996) and is exceeded only by the value for NGC 6752, another cluster with a purely blue HB.

Panels (c) and (d) in Figure 4 illustrate how larger amounts of helium mixing can shift the HB even further to the blue. In the  $\Delta X_{\text{mix}} = 0.10$  simulation of panel (c) most of the HB stars lie blueward of the instability strip, while in the  $\Delta X_{\text{mix}} = 0.20$  simulation in panel (d) the HB consists of a blue tail with a population of EHB stars at its hot end. The mean increase in  $Y_{\text{env}}$  for these 2 simulations was  $\approx 0.07$  and  $\approx 0.20$ , respectively. We emphasize again that the simulations in Figure 4 were all computed for the same distribution of the Reimers mass loss parameter  $\eta_{\text{R}}$ .

In producing Figure 4 we assumed that all of the stars in each panel mix to the same depth  $\Delta X_{\text{mix}}$  along the RGB. This may not be the case in an actual cluster if the mixing is controlled by the stellar rotation rate  $\omega$ . One would expect the mixing currents in a more rapidly rotating red-giant star to penetrate more deeply and hence to dredge up more processed material to the surface. This might lead to a gradient in the extent of the mixing along the HB, with the hotter HB stars being more heavily mixed, as indicated

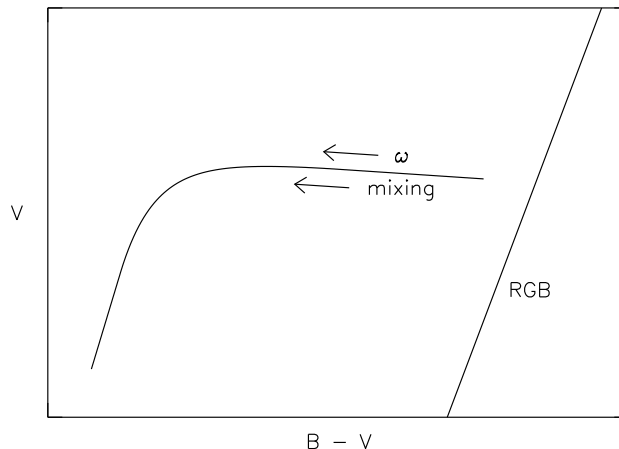


Fig. 5.— Schematic representation of the HB morphology produced by variable stellar rotation rates  $\omega$  and variable amounts of helium mixing.

schematically in Figure 5. In this case the BHB stars would be helium-rich compared to the RR Lyrae stars which, in turn, might be helium-rich compared to the red HB stars. Such rotationally driven mixing might thus lead to an upward tilt of the “horizontal” part of the HB with decreasing  $B - V$ , as has been found in the metal-rich clusters NGC 6388 and NGC 6441 by Piotto et al. (1997).

Figure 5 might be modified under some circumstances if there should be a threshold in the stellar rotation rate for helium mixing. If the rotation rate is too slow, the mixing currents might not be able to penetrate into the hydrogen shell before the nuclear burning sets up a gradient in the mean molecular weight  $\mu$  large enough to inhibit the mixing. This is more likely to occur at high metallicities where the hydrogen shell is steeper and where the timescale for setting up a  $\mu$  gradient is therefore shorter (Cavallo et al. 1997). Thus helium mixing in a metal-rich population might be confined to the more rapidly rotating giants. Such a threshold effect might lead to a bimodal HB morphology consisting of a red unmixed population and a blue mixed population, as shown schematically in Figure 6. This possibility may be relevant for understanding the bimodal HB morphologies of some globular clusters (Crocker, Rood, & O’Connell 1988; Borissova et al. 1997) as well as the more extreme bimodal morphologies found in metal-rich open clusters such as NGC 6791 (Liebert, Saffer, & Green 1994) and in elliptical galaxies where a hot HB population is believed to produce the UV upturn (Greggio & Renzini 1990; Dorman, O’Connell, & Rood 1995).

The above results support the possibility that stellar rotation might control the extent of mixing along the RGB as well as the well-known difference in HB morphology

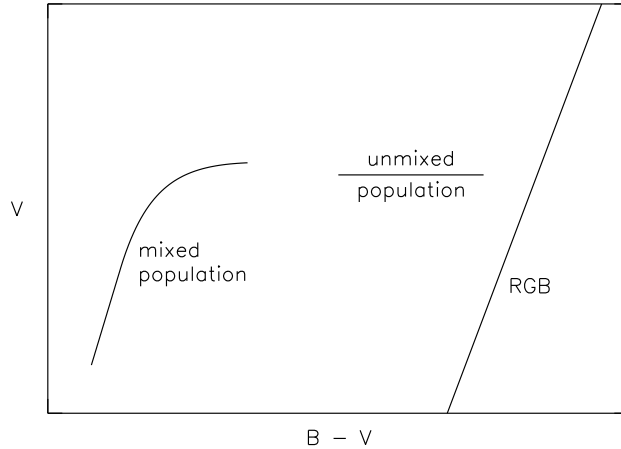


Fig. 6.— Schematic representation of the bimodal HB morphology produced by a red unmixed population and a blue mixed population.

between some 2nd parameter pairs of globular clusters (Renzini 1977; Fusi Pecci & Renzini 1978; Norris 1983, 1987; Peterson 1983; Buonanno, Corsi, & Fusi Pecci 1985; Kraft 1994; Kraft et al. 1995; Peterson, Rood, & Crocker 1995). Under this scenario globular clusters with rapid stellar rotation rates would mix helium along the RGB and hence have a bluer than expected HB morphology. Conversely, globular clusters with slower stellar rotation rates would mix little, if any, helium, and hence their HB morphology would approximate the canonical one. An example of this possibility is the 2nd parameter clusters M3 and M13, which some authors suggest may have similar ages (Paltrinieri et al. 1997 and references therein). Rotation may also be involved in producing the correlation between the relative number of BHB stars and the cluster central density (Fusi Pecci et al. 1993; Buonanno et al. 1997). As discussed by Buonanno et al. (1985), stellar encounters within the dense cores of such globular clusters might lead to a spin up of the red-giant envelope and hence to enhanced mass loss (see also Renzini 1983).

Helium mixing may also affect the properties of the RR Lyrae variables by increasing their luminosity and hence their predicted pulsation period  $P$ . This may be relevant for understanding the Sandage period-shift effect (Sandage 1982, 1990, 1993a). For example, a period shift of  $\Delta \log P = 0.065$  between M3 and M15 could be explained if the red-giant stars in M15 mix into the depth  $\Delta X_{\text{mix}} = 0.06$  (Sweigart 1997). Such mixing would have 2 important implications. First, it would increase  $Y_{\text{env}}$  in the RR Lyrae variables in M15 by 0.04 and consequently produce a  $Y - Z$  anticorrelation between these 2 clusters, as previously suggested by Sandage, Katem, & Sandage (1981) and Sandage (1982, 1990). Although such an anticorrelation between helium abundance and metallicity is counterintuitive, it

might arise during the RGB evolution if metal-poor giants mix more deeply (VandenBerg & Smith 1988). The second implication would be an increase in the luminosity of the RR Lyrae variables in M15 by  $\approx 0.2$  mag and consequently a steeper slope for the RR Lyrae luminosity-metallicity relation, as has also been advocated by Sandage (1982, 1990, 1993b). We note that relatively bright luminosities have been reported for the RR Lyrae variables in M15 by Bingham et al. (1984), Simon & Clement (1993) and Silbermann & Smith (1995). From a Baade-Wesselink analysis, Storm, Carney, & Latham (1994) have found that the RR Lyrae variables in another metal-poor cluster, M92, are  $\approx 0.2$  mag brighter than the field RR Lyrae variables of similar metallicity, although in this case the effect could be partially due to evolution away from the ZAHB (e.g., Rood & Crocker 1989). These results provide a potential means for testing the helium-mixed models. Before doing so, however, one needs to understand why the Baade-Wesselink luminosities for field RR Lyrae variables are systematically fainter than canonical HB models (e.g., Castellani & De Santis 1994) and to determine whether this systematic offset also applies to the cluster variables. In any case, the present results suggest that there may be a relationship between the observed abundance variations along the RGB and the pulsation properties of the RR Lyrae variables, as has also been noted by VandenBerg et al. (1996).

### 3.2. Low Gravities of the Blue HB Stars

A number of observational studies have shown that the surface gravities of the globular cluster BHB stars are lower than predicted by canonical stellar models (Crocker et al. 1988; Moehler, Heber, & de Boer 1995; de Boer, Schmidt, & Heber 1995; Moehler, Heber, & Rupprecht 1997b). The size of this discrepancy increases with  $\log T_{\text{eff}}$ , reaching  $\approx 0.3$  in  $\Delta \log g$  for  $4.3 > \log T_{\text{eff}} > 4.2$ . Curiously the EHB stars with  $\log T_{\text{eff}} > 4.3$  have gravities in good agreement with canonical theory. These results are illustrated in Figure 7, where we plot the observed gravities for the hot HB stars in a number of globular clusters together with a set of canonical HB and post-HB evolutionary tracks. Each track is represented by a series of dots spaced every  $5 \times 10^5$  yr along the evolution so that one can better compare the expected location of the models with the observational data.

Figure 7 raises some intriguing questions: does the structure of an HB star change in some basic way around  $\log T_{\text{eff}} = 4.3$ , and could such a change be related to the low observed gravities? Although perhaps a coincidence,  $\log T_{\text{eff}} = 4.3$  is approximately the temperature at which the hydrogen shell becomes an active energy source. Blueward of  $\log T_{\text{eff}} = 4.3$ , the envelope mass is insufficient to sustain an active hydrogen shell, while redward of this temperature the hydrogen shell makes an increasingly important contribution to the surface luminosity. The observed shift towards lower gravities at  $\log T_{\text{eff}} = 4.3$  may be an indication that the hydrogen shell turns on more strongly as one goes from the

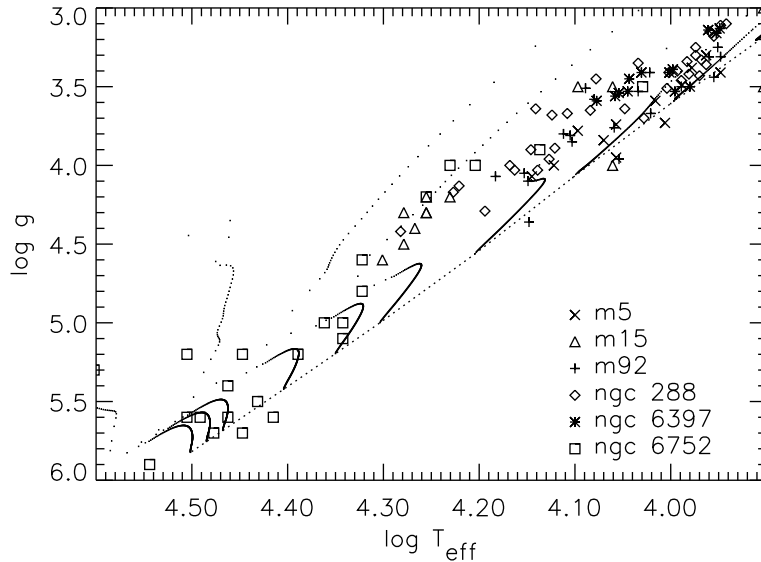


Fig. 7.— Comparison between canonical HB and post-HB evolutionary tracks and the observed gravities of the hot HB stars in a number of globular clusters. The dots along each track are separated by  $5 \times 10^5$  yr. Data are from Crocker et al. (1988), Moehler et al. (1995, 1997b) and de Boer et al. (1995). The dotted line indicates the ZAHB.

EHB to the BHB than predicted by canonical models. Some support for this suggestion is provided by the ultraviolet observations of the hot HB stars in M79 (Hill et al. 1992),  $\omega$  Cen (Whitney et al. 1994), and NGC 6752 (Landsman et al. 1996b) obtained with the Ultraviolet Imaging Telescope (Stecher et al. 1992). In each of these clusters the luminosity difference between the EHB and the BHB appears to be larger than expected from canonical models.

Crocker et al. (1988) and Rood & Crocker (1989) have discussed the effects of various HB parameters on the predicted gravities. The only change they could identify which would reproduce the observed gravities on both the EHB and BHB was an enhancement in the envelope helium abundance (see also Gross 1973). Changes in the CNO abundance, mass loss and age do not work. Similarly rotation is not a solution if its only effect is to increase the core mass at the helium flash.

The above considerations suggest that helium mixing might be able to explain the low gravities of the BHB stars. We explore this possibility in Figures 8 and 9, where we plot the observational data from Figure 7 together with the helium-mixed tracks for  $\Delta X_{\text{mix}} = 0.10$  and  $0.20$ , respectively. The gravities of the tracks in Figure 8 agree well with the observational data over the temperature range  $4.1 > \log T_{\text{eff}} > 4.0$  but are

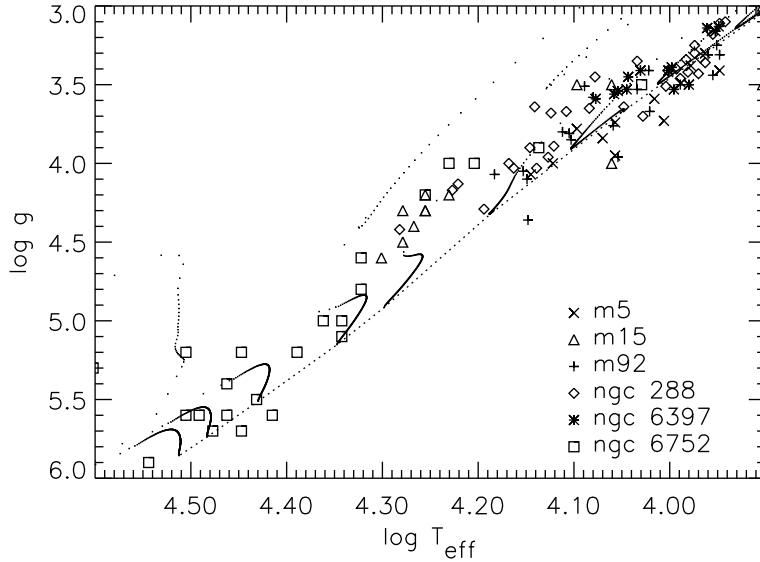


Fig. 8.— Same as Figure 7 except for helium-mixed tracks with  $\Delta X_{\text{mix}} = 0.10$ .

still too large for  $4.3 > \log T_{\text{eff}} > 4.2$ . This latter discrepancy can be removed by more extensive mixing, as shown in Figure 9, but then the predicted gravities become too low for  $4.1 > \log T_{\text{eff}} > 4.0$ . These results suggest that the observed variation of  $\log g$  with  $\log T_{\text{eff}}$  can be understood if there is a gradient in the amount of helium mixing, with the hotter BHB stars being more extensively mixed. Note that this is in the same sense as is needed to produce a bluer HB morphology. For the present sequences this would imply a variation in  $Y_{\text{env}}$  from  $\approx 0.32$  for  $4.1 > \log T_{\text{eff}} > 4.0$  to  $\approx 0.44$  for  $4.3 > \log T_{\text{eff}} > 4.2$ . In the following subsection we will see that an even larger enhancement of  $Y_{\text{env}}$  may be necessary to explain the EHB stars.

The helium-mixed models have lower gravities because they are more luminous. This prediction can be tested by comparing the bolometric luminosities of the helium-mixed models with the observed luminosities along the BHB, although this test would be affected by uncertainties in the distance modulus and reddening, large bolometric corrections to the visual data, small number of blue standards for photometric calibration, etc. In addition, one could use the luminosity difference between the EHB and the BHB, which is sensitive to the envelope helium abundance, to differentiate between the canonical and helium-mixed models. It would also be important to continue spectroscopic studies of the BHB stars to look for cases where diffusion has not affected the surface composition (Crocker, Rood, & O’Connell 1986; Crocker & Rood 1988; Corbally, Gray, & Philip 1997).

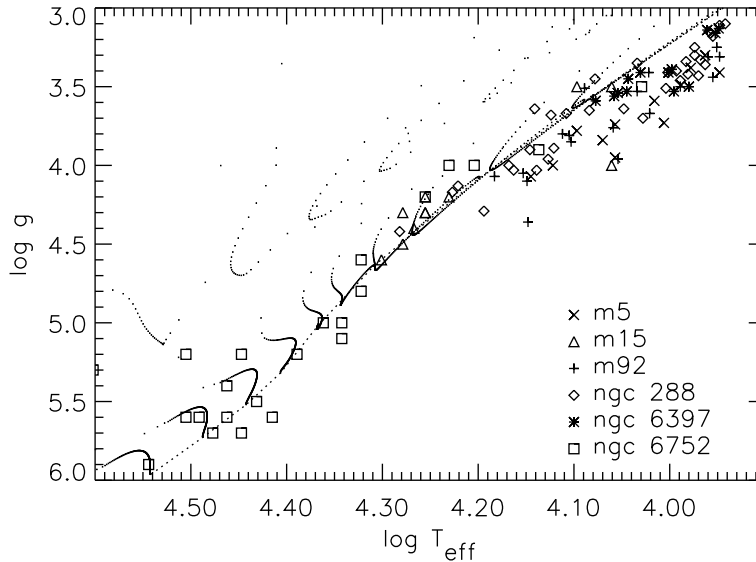


Fig. 9.— Same as Figure 7 except for helium-mixed tracks with  $\Delta X_{\text{mix}} = 0.20$ .

### 3.3. Origin of the Extreme HB Stars

The origin of the EHB stars found in the field and in some globular clusters has been a puzzle for some time. Various explanations have been offered, including binary-star scenarios involving mergers (Iben & Tutukov 1984; Iben 1990) and mass transfer (Mengel, Norris, & Gross 1976) as well as single-star scenarios involving unusually large mass loss along the RGB (Sweigart, Mengel, & Demarque 1974; D’Cruz et al. 1996). The binary-star scenarios generally predict a wide range in the luminosity of the EHB stars which appears to be inconsistent with the observed luminosities of the hot HB stars in the globular clusters (see, e.g., Landsman et al. 1996b). For this reason we will focus our attention on the single-star scenario.

The principal difficulty of the single-star scenario is the problem of fine tuning the mass loss along the RGB to produce the very small envelope masses ( $\approx 10^{-2} M_{\odot}$ ) required for the high effective temperatures ( $> 20,000 \text{ K}$ ) of the EHB stars. Too much mass loss and a star will bypass the HB phase and die as a helium white dwarf; too little mass loss and a star will lie too red along the HB. We will now illustrate this problem with some new canonical calculations. Following this, we will show how helium mixing may offer a possible solution because it permits substantially larger envelope masses.

Figures 10 and 11 show the tracks for two canonical sequences during the evolution up the RGB and through the helium flash to the ZAHB. The mass loss parameter  $\eta_{\text{R}}$  for the

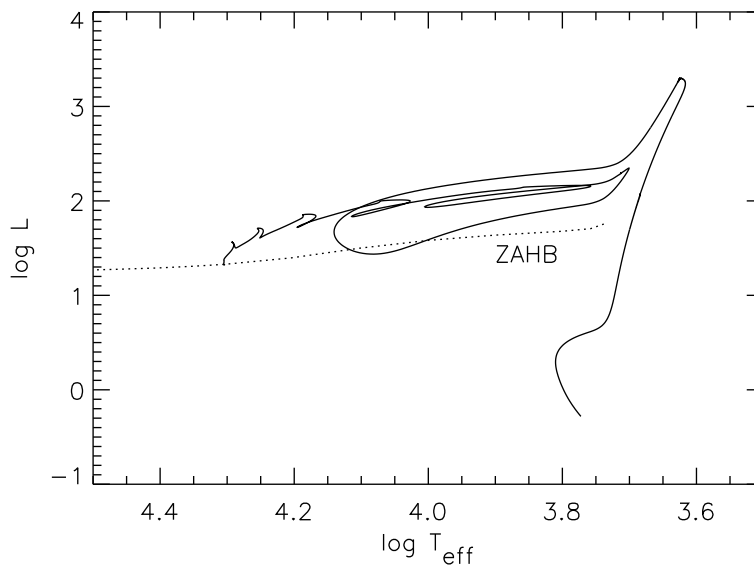


Fig. 10.— Canonical evolution from the RGB through the helium flash to the ZAHB for the Reimers mass loss parameter  $\eta_R = 0.653$ .

sequence in Figure 10 was adjusted to give a ZAHB effective temperature near the cool end of the EHB. Due to its high mass loss rate this sequence was starting to evolve away from the RGB when the helium flash began. The gyrations in the track during the subsequent evolution to the ZAHB are caused by the main and secondary flashes which occur in the core as the helium burning progresses towards the center. This aspect of the helium flash is discussed more fully by Mengel & Sweigart (1981) and Sweigart (1994).

The sequence in Figure 11 was computed with a higher mass loss rate in order to study the hotter EHB stars. In this case the models evolved off the RGB to very high effective temperatures ( $\log T_{\text{eff}} \approx 5.0$ ) before undergoing the helium flash. Following a number of flash-induced gyrations, this sequence settled onto the hot end of the EHB. The ZAHB envelope masses of the sequences in Figures 10 and 11 were only  $0.03$  and  $0.001 M_{\odot}$ , respectively, as compared to a total mass loss along the RGB of  $\approx 0.3 M_{\odot}$ . This shows that the ZAHB envelope mass must fall within a very narrow range compared to the total mass loss in order to produce an EHB star.

Castellani & Castellani (1993) have recently shown that the helium flash can be further delayed until a star is descending the white dwarf cooling curve if the mass loss is sufficiently large. This possibility has been explored by D’Cruz et al. (1996), who suggested that the fine tuning problem might be avoided if the EHB stars were the progeny of such “hot helium flashers”. We examine this possibility in Figure 12, where we follow the evolution

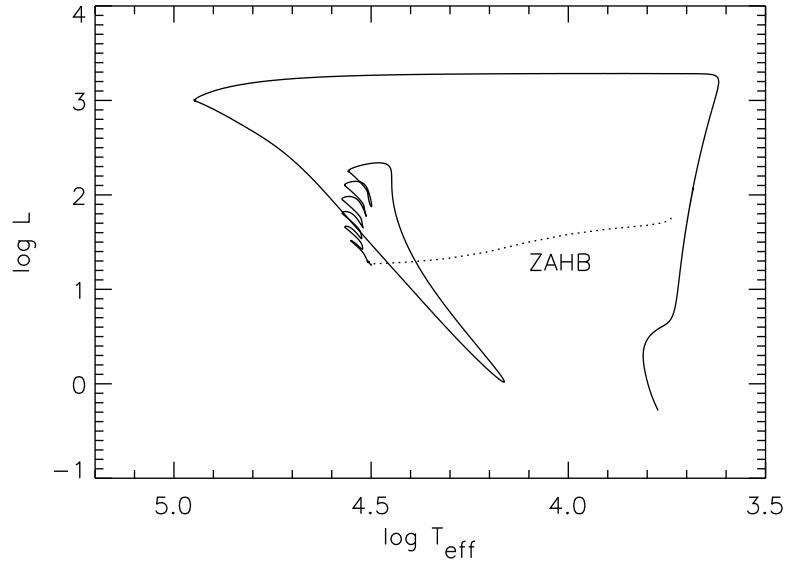


Fig. 11.— Canonical evolution from the RGB through the helium flash to the ZAHB for the Reimers mass loss parameter  $\eta_R = 0.740$ .

of a representative star from the white dwarf cooling curve to the ZAHB. The helium flash in this case is more complicated than in Figures 10 and 11. At the main flash peak, the helium-burning luminosity reached  $10^{10} L_{\odot}$ , as is typical for the helium flash in a low-mass star. Ordinarily the flash convection produced by such high burning rates does not reach the hydrogen shell, and consequently no hydrogen is mixed from the envelope into the core. In contrast, the flash convection in Figure 12 penetrated into the envelope and rapidly mixed hydrogen into the hot helium-burning interior. This hydrogen mixing is analogous to the mixing that sometimes occurs during a final helium-shell flash (see Iben 1995 and references therein) and should be a general characteristic of any helium flash that begins on the white dwarf cooling curve.

The penetration of the flash convection into the envelope is shown more clearly in Figure 13. At its maximum extent, the flash convection engulfed nearly 90% of the envelope hydrogen, implying a corresponding decrease in the envelope mass at the ZAHB phase. Some of the helium and carbon carried out by the flash convection was subsequently dredged up to the surface when a convective envelope formed during the rapid redward excursion of the track following the main flash. The surface composition after this dredge-up was 81% helium and 3% carbon by mass. The present calculations do not include the energy that is released as the hydrogen is mixed inward and burned, and consequently they may underestimate the surface composition change. It is possible that all of the residual envelope hydrogen may be consumed and that part, or all, of the carbon may be burned to

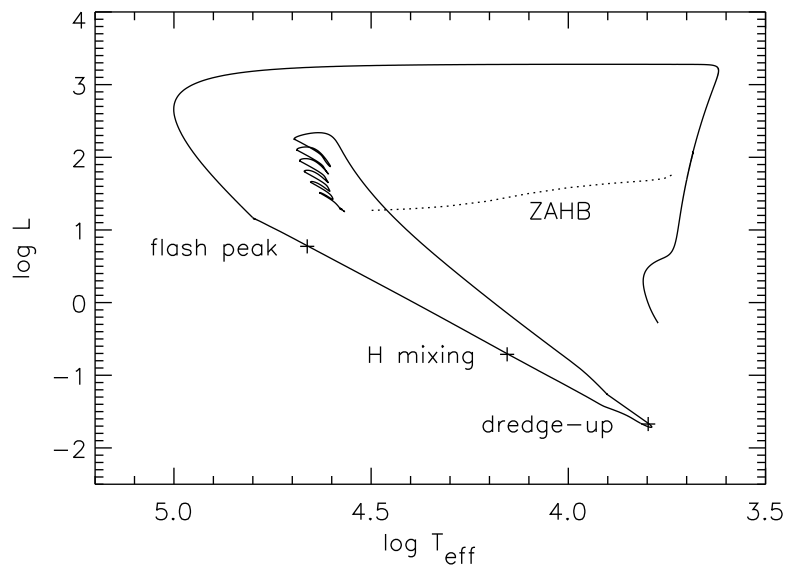


Fig. 12.— Canonical evolution from the RGB through the helium flash to the ZAHB for the Reimers mass loss parameter  $\eta_R = 0.750$ . The 3 plus signs denote the peak of the main helium flash, the onset of hydrogen mixing into the core and the dredge-up of helium and carbon-rich material by the convective envelope.

nitrogen.

The present results indicate that “hot helium flashers” are not the progenitors of the EHB stars both because the predicted surface abundances seem more appropriate for sdO than sdB stars and because the predicted ZAHB effective temperatures ( $\log T_{\text{eff}} \approx 4.6$ ) are hotter than those observed in most EHB stars. The evolution in Figure 12 may, however, be relevant for understanding the origin of the very helium-rich sdO stars discussed by Lemke et al. (1997).

Helium mixing offers an alternative scenario for producing the EHB stars. In Sec. 3.1 we saw how substantial helium mixing could move a star onto the hot end of the HB. However, we have not yet determined if helium mixing can overcome the “fine tuning” problem discussed previously. To address this point, we plot the envelope masses of both the canonical and helium-mixed models as a function of the ZAHB effective temperature in Figure 14. We see that EHB stars which have undergone substantial helium mixing have considerably larger envelope masses than their canonical counterparts and therefore require much less fine tuning of the mass loss. Such models also have a high envelope helium abundance, which may be important for understanding the high helium abundances of the sdO progeny of the EHB stars, as we will discuss in the following subsection.

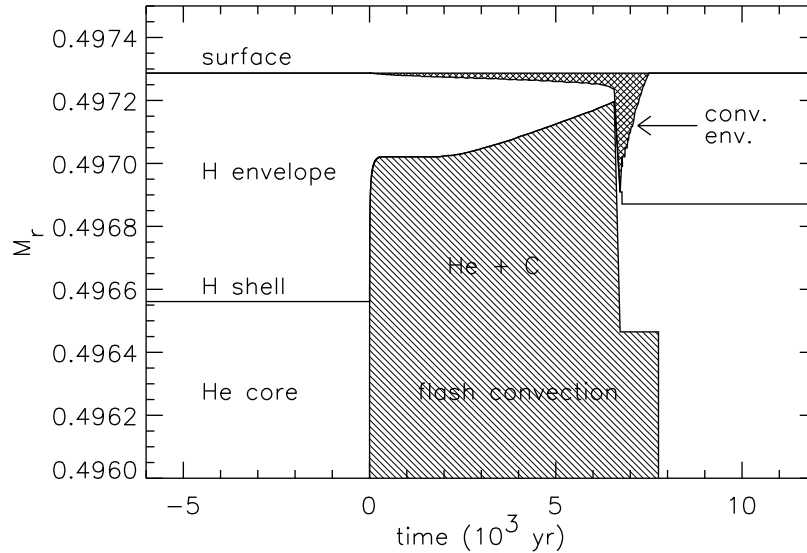


Fig. 13.— Time dependence of the mass coordinate  $M_r$  in solar units at the center of the hydrogen shell, the outer edge of the flash convection zone, the inner edge of the convective envelope and the stellar surface during the helium flash shown in Figure 12. The zero-point of the timescale corresponds to the peak of the main helium flash. Shaded areas are convective.

There are some observational tests of this helium-mixing scenario. Canonical models predict an abrupt increase in the surface luminosity at the end of the EHB phase as the helium burning shifts outward from the center to a shell. Observationally this should appear as a gap between the EHB and post-EHB stars in either the  $\log L - \log T_{\text{eff}}$  or  $\log g - \log T_{\text{eff}}$  diagram. The helium-mixed models predict a significantly larger gap, since the hydrogen shell in these models becomes active during the transition to helium-shell burning as a consequence of the larger envelope mass. This effect can be seen by comparing the tracks in Figure 9 with those in Figure 7. Although the statistics are uncertain, there is an indication that the luminosity gap between the EHB and post-EHB stars in NGC 6752 may be larger than expected from canonical models (Landsman et al. 1996b). For these reasons it would be important to study the separation between the field EHB and post-EHB stars in the  $\log g - \log T_{\text{eff}}$  diagram, where the statistics are better defined (Saffer 1997). Such a study might be complicated, however, by the fact that the abundance variations in the halo field RGB stars are not as pronounced as in the globular cluster giants (Suntzeff 1993; Kraft 1994).

One should also search for EHB and post-EHB stars where diffusion may not have modified the surface composition. For example, Moehler, Heber, & Durrell (1997a) have found a very hot, helium-rich ( $Y \approx 0.9$ ) EHB star in M15, while Landsman et al. (1996a)

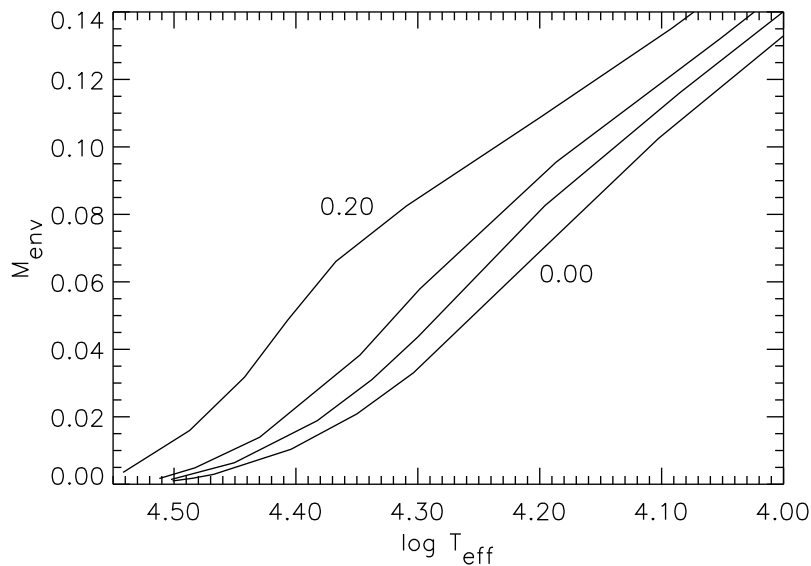


Fig. 14.— Dependence of the envelope mass  $M_{\text{env}}$  in solar units on  $\log T_{\text{eff}}$  at the ZAHB phase. Curves are given for canonical models (labeled 0.00) and for helium-mixed models with  $\Delta X_{\text{mix}} = 0.05, 0.10$  and  $0.20$  (upper curves).

have reported on a UV-bright (and possibly post-EHB) star in  $\omega$  Cen with  $Y \approx 0.7$ .

### 3.4. Evolutionary Status of the sdO Stars

A number of evolutionary channels probably contribute to the field sdO population. The most luminous, lowest gravity sdO stars appear to be on post-asymptotic-giant-branch (AGB) evolutionary tracks, while some of the most helium-rich (and C + N enhanced) sdO stars may have undergone a delayed helium flash as in Figure 12. It is also likely that some sdO stars may have evolved from the EHB, as suggested by Wesemael et al. (1982). However, two objections have been raised against this possibility: 1) that post-EHB evolutionary tracks do not cover the region of the  $\log g - \log T_{\text{eff}}$  diagram occupied by the sdO stars (Thejll 1994) and 2) that the hydrogen-rich atmosphere of an sdB star cannot be easily transformed into the helium-rich atmosphere of an sdO star. We will now consider whether the helium-mixed models can help to resolve these objections.

We address the first objection in Figure 15, where we plot the 3 EHB and post-EHB evolutionary tracks with the most extensive helium mixing computed thus far, i.e.,  $\Delta X_{\text{mix}} = 0.20$ ,  $Y_{\text{env}} \approx 0.6$ . Each track is again represented by a series of dots separated by an interval of  $5 \times 10^5$  yr so that one can see where these models spent the most time

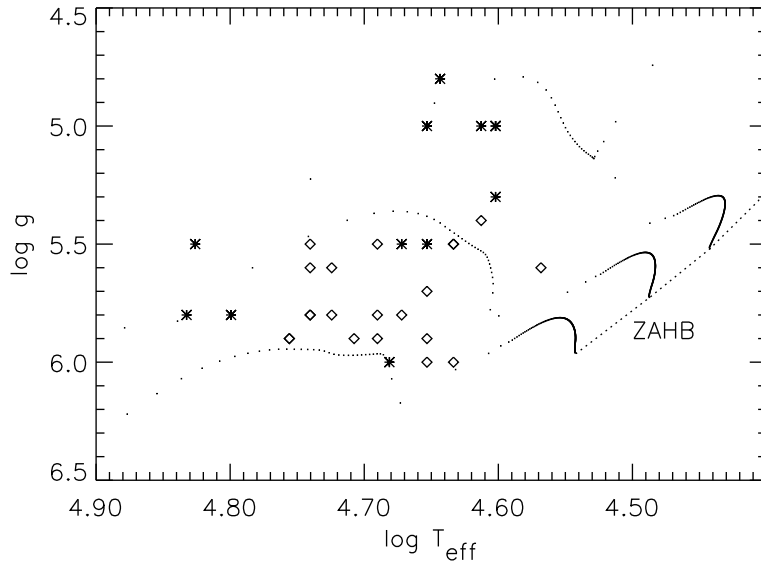


Fig. 15.— Comparison between the helium-mixed EHB and post-EHB evolutionary tracks for  $\Delta X_{\text{mix}} = 0.20$  and the observed gravities of the helium-rich sdO stars. Data are from Dreizler et al. (1990) (asterisks) and Thejll (1994) (diamonds).

in the  $\log g - \log T_{\text{eff}}$  diagram. The data for the helium-rich sdO stars in Figure 15 are taken from Dreizler et al. (1990) and Thejll (1994). We see that these helium-rich post-EHB tracks nicely bound the observed location of the sdO stars, including the sdO stars having the highest surface gravities. This suggests that the highest gravity sdO stars do not necessarily lie on the helium-burning main sequence.

For comparison we plot 3 canonical EHB and post-EHB tracks in Figure 16. These tracks are the hottest ones that we could compute before the models underwent the extensive flash-induced mixing shown in Figures 12 and 13. While the post-EHB tracks in Figure 16 pass through much of the sdO domain, they cannot explain the highest gravity sdO stars. Moreover, these canonical tracks have very small ZAHB envelope masses ( $< 0.003 M_{\odot}$ ) and consequently suffer from the fine tuning problem discussed in the previous subsection.

The helium-mixed models can straightforwardly overcome the second objection against the post-EHB scenario for the sdO stars because the envelopes of these models are already helium-rich. All that is required is for the outermost layers where helium has been depleted by diffusion during the sdB phase to be either removed or mixed with the helium-rich interior. There are 3 ways in which this could be accomplished. First, a hot stellar wind might remove the thin hydrogen-rich surface veneer. This possibility differs from the suggestion of MacDonald & Arrieta (1994), who required that the stellar wind

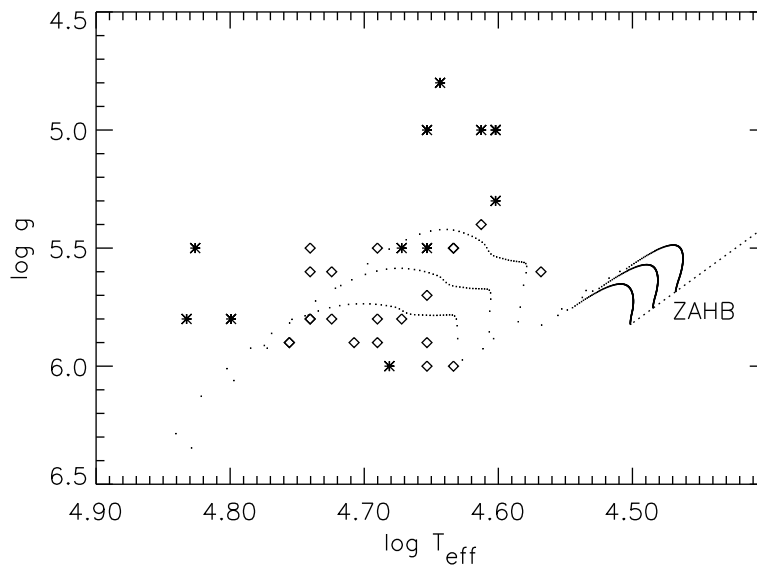


Fig. 16.— Comparison between canonical EHB and post-EHB evolutionary tracks and the observed gravities of the helium-rich sdO stars. Data are the same as in Figure 15.

remove all of the envelope in order to expose the helium-rich core. Secondly, Groth, Kudritzki, & Heber (1985) have suggested that HeII/HeIII convection might mix the outermost layers if  $Y_{\text{env}} > 0.5$ . This condition is fulfilled by the helium-mixed models in Figure 15. Thirdly, some post-EHB stars experience helium-shell flashes during which they make brief excursions back to the AGB (Caloi 1989). The convective envelope that develops at that time would mix the envelope and therefore remove any vestige of the prior diffusion.

We conclude that the helium-mixed sequences such as those in Figure 15 support the suggestion of an evolutionary link between the sdO and sdB stars.

#### 4. Summary

The helium-mixing scenario outlined in this paper predicts that the effects of helium mixing should become more pronounced as one goes blueward along the HB. Thus the RR Lyrae stars should be affected the least, the BHB stars more so, and the EHB stars the most. This trend is in the same sense as was needed to account for a number of observational results. Relatively small amounts of helium mixing can reproduce the 2nd parameter effect and lower the globular cluster ages derived from the  $\Delta V$  method. Somewhat more mixing is needed to explain the low gravities of the BHB stars, while extensive mixing seems necessary to explain the high effective temperatures of the sdB stars and the high helium abundances

of their sdO progeny. Clearly much observational and theoretical work remains to be done to explore these implications of helium mixing and to determine if such mixing actually occurs in low-mass red-giant stars.

We conclude with a brief summary of the main points of this paper:

1. The observed abundance variations, particularly those involving Al, suggest that low-mass red-giant stars may be mixing helium from the top of the hydrogen shell into the envelope.
2. Noncanonical models with helium mixing have a higher envelope helium abundance and suffer greater mass loss along the RGB.
3. Helium mixing would mimic age as the 2nd parameter and would reduce the globular cluster age derived from the  $\Delta V$  method.
4. Helium mixing produces a hotter HB morphology, thereby making it easier to explain the EHB populations observed in different stellar systems.
5. BHB models with helium mixing have lower surface gravities than canonical models.
6. Helium mixing might explain the high helium abundances of some helium-rich sdO stars.

The author is indebted to M. Catelan for many insightful comments, for a critical reading of this paper, and for computing the HB simulations in Figure 4. The author also gratefully acknowledges R. Cavallo for preparing Figure 1. This research was supported in part by NASA grant NAG5-3028

#### REFERENCES:

- Arribas, S., Caputo, F., & Martinez-Roger, C. 1991, *A&AS*, 88, 19  
 Bell, R. A., & Dickens, R. J. 1980, *ApJ*, 242, 657  
 Bell, R. A., Dickens, R. J., & Gustafsson, B. 1979, *ApJ*, 229, 604  
 Bingham, E. A., Cacciari, C., Dickens, R. J., & Fusi Pecci, F. 1984, *MNRAS*, 209, 765  
 Borissova, J., Catelan, M., Spassova, N., & Sweigart, A. V. 1997, *AJ*, 113, 692  
 Briley, M. M., Bell, R. A., Hoban, S., & Dickens, R. J. 1990, *ApJ*, 359, 307  
 Buonanno, R. 1993, in *ASP Conf. Series 48, The Globular Cluster- Galaxy Connection*, ed. G. H. Smith & J. P. Brodie (San Francisco: ASP), 131

- Buonanno, R., Corsi, C., Bellazzini, M., Ferraro, F. R., & Fusi Pecci, F. 1997, *AJ*, 113, 706
- Buonanno, R., Corsi, C. E., & Fusi Pecci, F. 1985, *A&A*, 145, 97
- Buonanno, R., Corsi, C. E., & Fusi Pecci, F. 1989, *A&A*, 216, 80
- Caloi, V. 1989, *A&A*, 221, 27
- Carbon, D. F., Langer, G. E., Butler, D., Kraft, R. P., Suntzeff, N. B., Kemper, E., Trefzger, C. F., & Romanishin, W. 1982, *ApJS*, 49, 207
- Castellani, M., & Castellani, V. 1993, *ApJ*, 407, 649
- Castellani, V., & De Santis, R. 1994, *ApJ*, 430, 624
- Catelan, M. 1996, private communication
- Cavallo, R. M., Sweigart, A. V., & Bell, R. A. 1996, *ApJ*, 464, L79
- Cavallo, R. M., Sweigart, A. V., & Bell, R. A. 1997, in preparation
- Chaboyer, B., Demarque, P., & Sarajedini, A. 1996, *ApJ*, 459, 558
- Corbally, C. J., Gray, R. O., & Philip, A. G. D. 1997, this conference
- Crocker, D. A., & Rood, R. T. 1988, in *IAU Sym. 126, Globular Cluster Systems in Galaxies*, ed. J. E. Grindlay & A. G. D. Philip (Dordrecht: Kluwer), 509
- Crocker, D. A., Rood, R. T., & O'Connell, R. W. 1986, *ApJ*, 309, L23
- Crocker, D. A., Rood, R. T., & O'Connell, R. W. 1988, *ApJ*, 332, 236
- D'Cruz, N. L., Dorman, B., Rood, R. T., & O'Connell, R. W. 1996, *ApJ*, 466, 359
- de Boer, K. S., Schmidt, J. H. K., & Heber, U. 1995, *A&A*, 303, 95
- Denisenkov, P. A., & Denisenkova, S. N. 1990, *Soviet Astron. Lett.*, 16, 275
- Dorman, B., O'Connell, R. W., & Rood, R. T. 1995, *ApJ*, 442, 105
- Dreizler, S., Heber, U., Werner, K., Moehler, S., & de Boer, K. S. 1990, *A&A*, 235, 234
- Fusi Pecci, F., Ferraro, F. R., Bellazzini, M., Djorgovski, S., Piotto, G., & Buonanno, R. 1993, *AJ*, 105, 1145
- Fusi Pecci, F., Ferraro, F. R., Crocker, D. A., Rood, R. T., & Buonanno, R. 1990, *A&A*, 238, 95
- Fusi Pecci, F., & Renzini, A. 1976, *A&A*, 46, 447
- Fusi Pecci, F., & Renzini, A. 1978, in *IAU Sym. 80, The HR Diagram*, ed. A. G. D. Philip & D. S. Hayes (Dordrecht: Reidel), 225
- Greggio, L., & Renzini, A. 1990, *ApJ*, 364, 35
- Gross, P. G. 1973, *MNRAS*, 164, 65
- Groth, H. G., Kudritzki, R. P., & Heber, U. 1985, *A&A*, 152, 107
- Hill, R. S., et al. 1992, *ApJ*, 395, L17
- Hurley, D. J. C., Richer, H. B., & Fahlman, G. G. 1989, *AJ*, 98, 2124
- Iben, I., Jr. 1990, *ApJ*, 353, 215
- Iben, I., Jr. 1995, *Physics Reports*, 250, 1
- Iben, I., Jr. & Renzini, A. 1984, *Physics Reports*, 105, 329
- Iben, I., Jr., & Tutukov, A. V. 1984, *ApJS*, 54, 335
- Kraft, R. P. 1994, *PASP*, 106, 553
- Kraft, R. P., Sneden, C., Langer, G. E., & Shetrone, M. D. 1993, *AJ*, 106, 1490
- Kraft, R. P., Sneden, C., Langer, G. E., Shetrone, M. D., & Bolte, M. 1995, *AJ*, 109, 2586

- Kraft, R. P., Sneden, C., Smith, G. H., Shetrone, M. D., Langer, G. E., & Pilachowski, C. A. 1997, *AJ*, 113, 279
- Landsman, W. B., Crotts, A. P. S., Hubeny, I., Lanz, T., O'Connell, R. W., Whitney, J., & Stecher, T. P. 1996a, in *ASP Conf. Series 99, Cosmic Abundances*, ed. S. S. Holt & G. Sonneborn (San Francisco: ASP), 199
- Landsman, W. B., et al. 1996b, *ApJ*, 472, L93
- Langer, G. E., & Hoffman, R. D. 1995, *PASP*, 107, 1177
- Langer, G. E., Hoffman, R., & Sneden, C. 1993, *PASP*, 105, 301
- Lemke, M., Heber, U., Napiwotzki, R., Dreizler, S., & Engels, D. 1997, this conference
- Liebert, J., Saffer, R. A., & Green, E. M. 1994, *AJ*, 107, 1408
- MacDonald, J., & Arrieta, S. S. 1994, in *Hot Stars in the Galactic Halo*, ed. S. J. Adelman, A. R. Upgren, & C. J. Adelman (Cambridge: Cambridge Univ. Press), 238
- Mengel, J. G., Norris, J., & Gross, P. G. 1976, *ApJ*, 204, 488
- Mengel, J. G., & Sweigart, A. V. 1981, in *IAU Colloq. 68, Astrophysical Parameters for Globular Clusters*, ed. A. G. D. Philip & D. S. Hayes (Dordrecht: Reidel), 277
- Moehler, S., Heber, U., & de Boer, K. S. 1995, *A&A*, 294, 65
- Moehler, S., Heber, U., & Durrell, P. R. 1997a, *A&A*, 317, L83
- Moehler, S., Heber, U., & Rupprecht, G. 1997b, *A&A*, in press
- Norris, J. 1983, *ApJ*, 272, 245
- Norris, J. 1987, *ApJ*, 313, L65
- Norris, J. E., & Da Costa, G. S. 1995, *ApJ*, 441, L81
- Paltrinieri, B., et al. 1997, this conference
- Peterson, R. C. 1983, *ApJ*, 275, 737
- Peterson, R. C., Rood, R. T., & Crocker, D. A. 1995, *ApJ*, 453, 214
- Piotto, G., et al. 1997, in *Advances in Stellar Evolution*, ed. R. T. Rood & A. Renzini (Cambridge: Cambridge Univ. Press), in press
- Reimers, D. 1975, *Mem. Soc. Roy. Sci. Liege*, 6th Series, 8, 369
- Renzini, A. 1977, in *Advanced Stages in Stellar Evolution*, ed. P. Bouvier & A. Maeder (Sauverny: Geneva Obs.), 149
- Renzini, A. 1983, *Mem. S. A. It.*, 54, 335
- Rood, R. T., & Crocker, D. A. 1989, in *IAU Colloq. 111, The Use of Pulsating Stars in Fundamental Problems of Astronomy*, ed. E. G. Schmidt (Cambridge: Cambridge Univ. Press), 103
- Saffer, R. 1997, this conference
- Sandage, A. 1982, *ApJ*, 252, 553
- Sandage, A. 1990, *ApJ*, 350, 631
- Sandage, A. 1993a, *AJ*, 106, 687
- Sandage, A. 1993b, *AJ*, 106, 703
- Sandage, A., Katem, B., & Sandage, M. 1981, *ApJS*, 46, 41
- Silbermann, N. A., & Smith, H. A. 1995, *AJ*, 110, 704; erratum: 1996, *AJ*, 111, 567
- Simon, N. R., & Clement, C. M. 1993, *ApJ*, 410, 526

- Stecher, T. P., et al. 1992, *ApJ*, 395, L1
- Storm, J., Carney, B. W., & Latham, D. W. 1994, *A&A*, 290, 443
- Suntzeff, N. 1993, in *ASP Conf. Series 48, The Globular Cluster- Galaxy Connection*, ed. G. H. Smith & J. P. Brodie (San Francisco: ASP), 167
- Sweigart, A. V. 1994, in *Hot Stars in the Galactic Halo*, ed. S. J. Adelman, A. R. Upgren, & C. J. Adelman (Cambridge: Cambridge Univ. Press), 17
- Sweigart, A. V. 1997, *ApJ*, 474, L23
- Sweigart, A. V., & Mengel, J. G. 1979, *ApJ*, 229, 624
- Sweigart, A. V., Mengel, J. G., & Demarque, P. 1974, *A&A*, 30, 13
- Thejll, P. 1994, in *Hot Stars in the Galactic Halo*, ed. S. J. Adelman, A. R. Upgren, & C. J. Adelman (Cambridge: Cambridge Univ. Press), 197
- VandenBerg, D. A., Bolte, M., & Stetson, P. B. 1996, *ARA&A*, 34, 461
- VandenBerg, D. A., & Smith, G. H. 1988, *PASP*, 100, 314
- Wesemael, F., Winget, D. E., Cabot, W., van Horn, H. M., & Fontaine, G. 1982, *ApJ*, 254, 221
- Whitney, J. H., et al. 1994, *AJ*, 108, 1350